King Saud University

Arabian Journal of Chemistry

www.ksu.edu.sa
www.sciencedirect.com

ORIGINAL ARTICLE

Smart thermometer style sensor with volume readout and visualization for pH detection

Shenghai Zhang [a], Rui Wu [b],*, **Jiagen Lv [c],***

[a] *School of Chemistry and Chemical, Ankang University, An'kang, Shaanxi 725100, PR China*
[b] *Shaanxi key laboratory of catalysis, College of Chemical and Environment Science, Shaanxi University of Technology, Hanzhong, Shaanxi 723001, PR China*
[c] *School of Chemistry & Chemical Engineering, Shaanxi Normal University, Xi'an, Shaanxi 710119, PR China*

Abstract A novel visual volume-type hydrogel sensor like thermometer for pH response was developed. The multifunctional stimuli-responsive fluorescent hydrogel was fabricated by employing 5, 6-dicarboxylic fluorescein crosslinked partially ammoniated polyacrylamide (PAM). The polymer hydrogel was characterized with fluorescent inverted microscope (FIM) and scanning electron microscope (SEM), as well as N_2 adsorption–desorption analysis. The polymer hydrogel emitted fluorescence and exhibited volume phase transition (VPT) in response to pH in aqueous solution. The intelligent response hydrogel was put into an elaborately altered shower-like pipette with uniform holes in which the water can pass through without the swelling hydrogel. A visual thermometer style hydrogel sensor combination of chemical reaction, separation and detection was designed. It was accurately measure the volume of hydrogel instead of the pH value when response to different pH solution by reading the graduation with naked eye. Therefore, the challenge for direct measurement of hydrogel volume was overcome. Meanwhile, a scale bar was also designed to indicate pH according to the volume. We can directly read the pH from the bar, similar to a thermometer in daily life. The volume-type sensor paves the way for VPT hydrogel sensors with convenience, visualization, low-cost, portable, smartness and ease of operation.

1. Introduction

Materials, information and energy are the three pillars that underpin the edifice of human civilization. Substances are the material basis of the improvement in all the production and living standards of human beings. They also supports the progress of other new technologies and symbolize human civilization. As an important branch of the chemical discipline, materials such as hydrogel play significant role in scientific

* Corresponding authors.
E-mail address: hftffc@163.com (R. Wu).
Peer review under responsibility of King Saud University.

Production and hosting by Elsevier

research. The field of chemistry has become increasingly dependent on novel materials, including polymer hydrogels and nanomaterials (Ibrahim et al., 2019; Viran and Manish, 2016; Zhu et al., 2010; Askim et al., 2013; Markus et al., 2016; Shimanovich and Gedanken, 2016; Zhen et al., 2019; Si et al., 2019).

Hydrogel is multivariate polymer system with a three-dimensional crosslinked network structure and is used in modern sensing systems with superior performance (Chen et al., 2019; Shao et al., 2014). Similar to living creatures responding to environmental changes, polymer hydrogel can undergo conformational changes in response to external stimuli, showing great promise in developing intelligent or smart materials. Hydrogel have also received considerable attention as superabsorbent agents, sensors, actuators, tissue engineering scaffolds and drug delivery systems due to their unique advantages, including softness, smartness, flexibility, biocompatibility, and sensitive response (Wang et al., 2018; Zhu et al., 2016; Kehr, 2014; Gao et al., 2014; Wang et al., 2016; Carmen et al., 2019; Héloïse et al., 2013; Seddiki and Aliouche, 2017). If the polymer endowed with functional groups such as amino, carboxyl, thiol and fluorophore moieties, the hydrogel becomes responsive to physical, chemical or biochemical stimuli, including pH, ion concentration, temperature, light, or electromagnetic field, and a corresponding change occurs, such as swelling or shrinkage (Kuang et al., 2018; Jae et al., 2016; Cui et al., 2018; Sebastian et al., 2016).

Inspired by natural creatures, researchers have designed hydrogel sensors based on VPT in response to external stimuli (Li et al., 2015; Coukouma and Asher, 2018; Cheng et al., 2016; Cai et al., 2016; Su et al., 2017). To achieve greater flexibility for their applications, the current design trend in stimuli-responsive hydrogel which is towards the measurement of volume, namely, greater than a hundredfold changes in volume, based on absorption or release of solution accompanied by considerable swelling forces. However, there is a challenge associated with volume measurement. Hydrogels are different from liquids or solids with irregular morphology. Thus, it is difficult to directly measure the volume of hydrogel. Most hydrogel sensors rely on an accompanying instrument to indirectly measure an optoelectronic signal with smart transducer. In the present work, an elaborate graduated pipette similar to a thermometer is obtained. The volume of the hydrogel was readout with a sophisticated pipette by the naked eye. Therefore, a thermometer hydrogel sensor based on VPT in response to pH was designed.

As a typical polymer, PAM and fluorescein as a raw material for hydrogel synthesis were explored for pH-responsive sensors due to VPT (Gong et al., 2016; Wang et al., 2014. Yu et al., 2018; Deng et al., 2018; Mistlberger et al., 2015; Sun et al., 2016; Satyendra and Banshi, 2013). The introduction of carboxylic and amino groups in fluorescein units in the polymer chain may confer the hydrogel with pH sensitivity through protonation/deprotonation. The polymer hydrogel responded to pH, accompanied with a change in volume. The synthesis of hydrogel include three steps (Scheme 1). The frame of the whole paper as follow (Scheme 2).

2. Material and methods

2.1. Material

Acrylamide (C_3H_5NO), glycol (PEG), sodium hydroxide (NaOH), hydrochloric acid (HCl) and sodium hypochlorite (NaClO) were purchased Tianjin Kemiou Chemical Reagent Co., Ltd. Pyromellitic acid ($C_{10}H_6O_8$), Potassium persulfate (KPS), were produced from Xi'an Chemical Reagent Factory. Anhydrous ethanol (EtOH), acetic anhydride (Ac_2O), m-dihydroxybenzene ($C_6H_6O_2$), were purchased from Sinopharm Chemical Reagent Co., Ltd. All chemicals were analytical grade. Ultrapure water was prepared by a Millipore water purification system.

2.2. Synthesis of polymer hydrogel and parameter optimization

Acrylamide (AAM) is an excellent raw material for the synthesis of hydrogel. A total of 5.67 g of AAM, 0.1088 g of potassium persulfate (SBS) and 0.56 g of polyethylene glycol-6000 (PEG-6000) were mixed with 120 mL of ultrapure water to react for 2 h in a 250 mL beaker with stirring at 65 °C. Then, the obtained colloids were poured into anhydrous ethanol and washed three times. PAM was obtained as a white powder.

The amide groups in PAM can be converted to amino groups under certain conditions. Firstly, 2.2 g of NaOH was dissolved in NaClO solution in water, shaken strongly, and cooled at −10 °C∼-0 °C. Then, PAM was added to the solution and kept for 6 h. Ethanol was added to the mixture. A white colloidal precipitate appeared and was dissolved with 6 M of HCl. Ethanol was added again, and caky solids began to float on the water. The solid was dried to a constant weight at 50 °C in a vacuum oven.

Next, 1.2 g of the obtained solid was mixed with 30 mL of ethylene glycol and gradually heated to 110 °C, then 60 mg of 5,6-dicarboxyl fluorescein was added. Furthermore, the temperature was increased to 180 °C and maintained for 30 min. Then, the solid was placed in 1 M NaOH solution at 100 °C for 2 h. After that, it was washed with ethanol to remove free fluorescein. A fluorescent hydrogel was obtained and dried under a vacuum oven.

2.3. Character assay

The dry hydrogel was ground into powder. The structure and morphology of the hydrogel were analysed with a fluorescent inverted microscope (FIM) and scanning electron microscope (SEM) at a voltage of 200 kV to investigate its properties. The swelling, adsorption, regeneration and reusability performances are significant factors for hydrogel. The swelling rate of the hydrogel in terms of weight was measured. Nitrogen adsorption–desorption isotherms for hydrogel were measured by using a Quantachrome ASIQ gas sorption model at 77 K. Before the adsorption measurements, all hydrogel were dried and out-gassed for 6 h at 200 ℃ in the degas port of the adsorption instrument. The degassing was performed at 200 °C for 3 h. Nitrogen is widely employed as an adsorbate because of its inert nature.
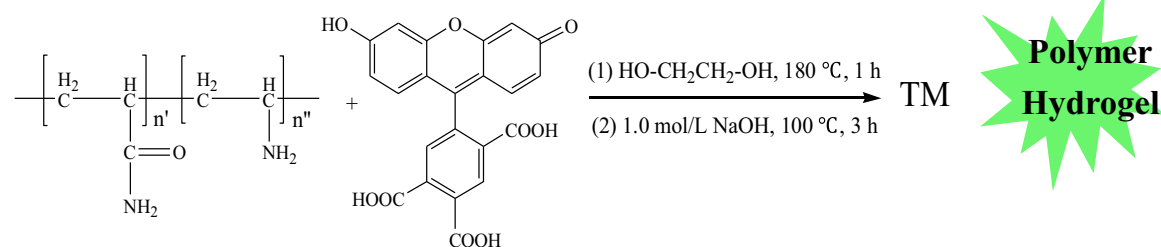
Step1
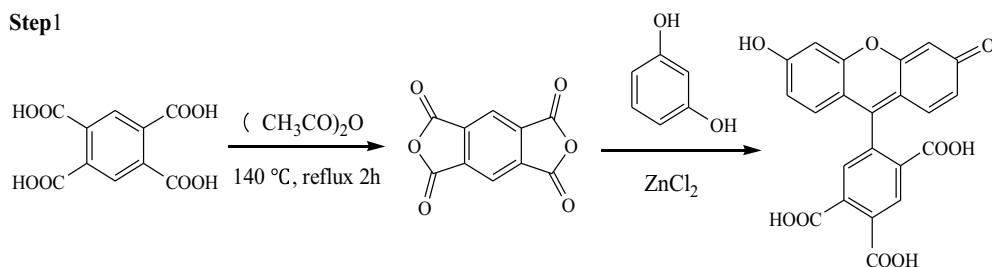
Step2
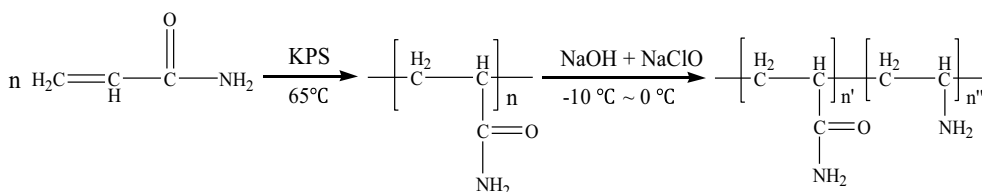
Step3

Scheme 1   The synthesis of hydrogel.

Because of the difficulty in measuring the volumes of a 3D irregularly dried or fully swelled hydrogel, the apparent swelling rate was measured according to the subsequent pH sensor establishment. A certain amount of dry hydrogel was weighed accurately, placed into a 10 mL pipette with a number of small holes uniform on the wall and immersed in distilled water. After several minutes, the pipette was removed and weighed to calculate the swelling rate. The hydrogel was also investigated for fluorescence behaviour.

2.4. The fabrication of a fluorescent polymer hydrogel sensor for pH detection

To measure the change in volume that occurred in response to pH, a thermometer-type pH sensor was developed. A 5 mL pipette with a number of uniform holes on the wall made by laser engraving was used, and the bottom of the pipette was sealed with cotton. The pipette was 0.5 cm in diameter and the minimum scale of the pipette was 50 µL. Water can penetrate the holes with a diameter of 0.8 mm freely, but the swelling hydrogel kept in the pipette. The solution of the sample consisted of hydrochloric acid and sodium hydroxide, and the pH range from 3 to 10. After 10 min, we can accurately and conveniently record the volume change based on the grad-

uation of the pipette with the naked eye. Following the same procedure, different pH values of the solution were investigated.

2.5. The fabrication of a scale bar

Convenience, visualization and smartness are popular pursuits for sensor. The ability to directly read the pH sensor with the naked eye instead of the volume would be a welcome development. For this purpose, a scale bar was prepared by translating the volume graduations into pH. The scale of the graduated pipette not only shows the volume of the hydrogel but also represents the corresponding pH value. Each scale was marked with a pH value similar to a thermometer.

3. Results

3.1. Synthesis and optimization of parameters

The fluorescent hydrogel was synthesized with 5,6-dicarboxyl fluorescein and partially ammoniated PAM. The dried and water-swelled hydrogels are shown (Fig. 1). The dried hydrogel particles were golden yellow under ultraviolet light. The
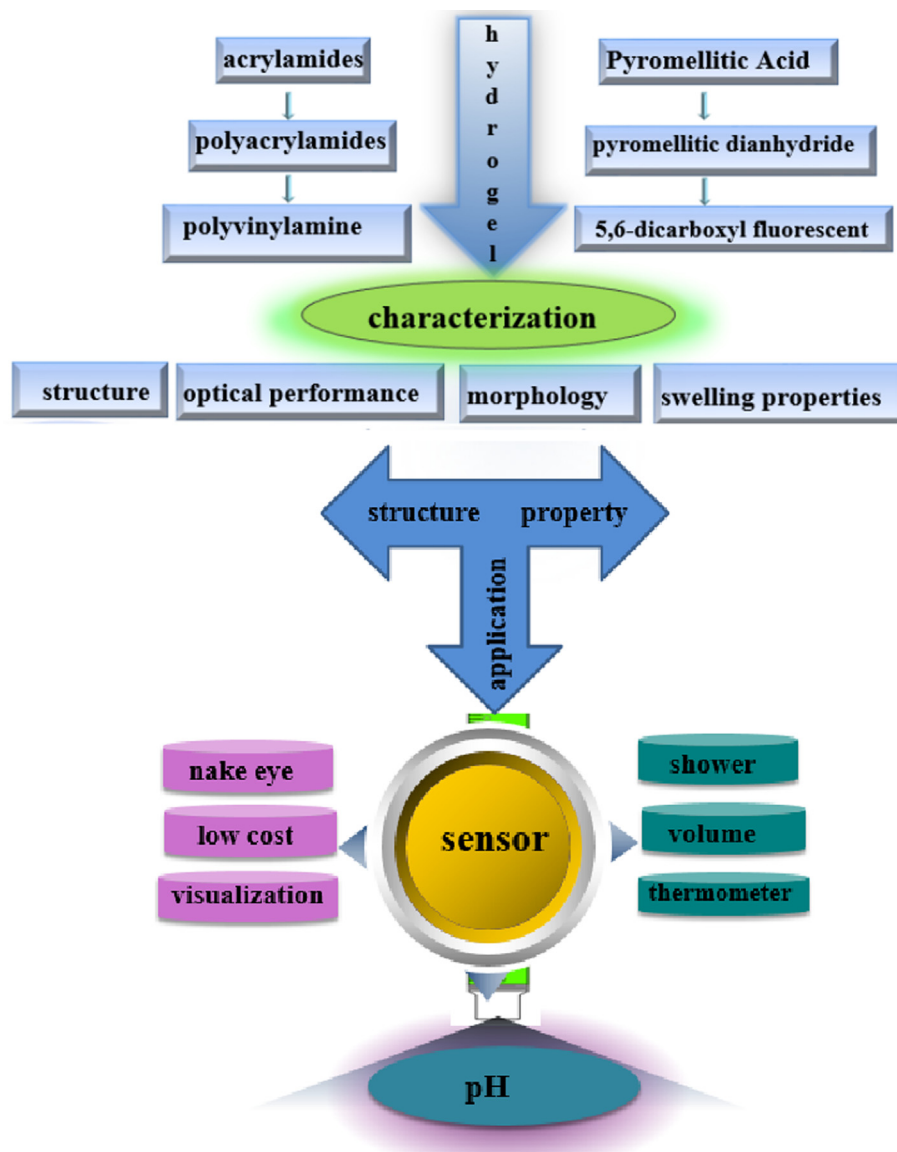
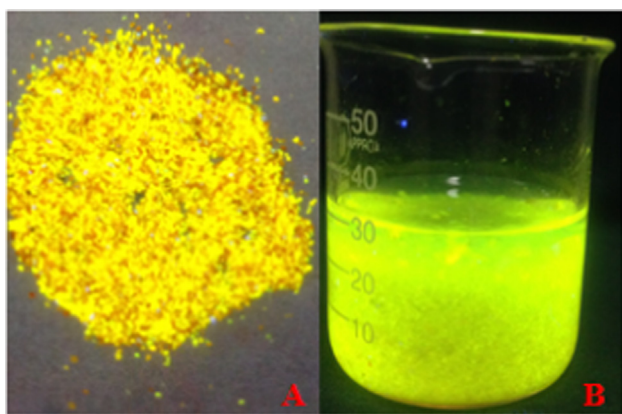**Scheme 2** The design of the hydrogel sensor and application.

Fig. 1 The hydrogel under ultraviolet light; (A) dried and (B) swelling hydrogel in water.

swelled hydrogel was kelly green. The parameters for the synthesis temperature and time were discussed (Fig. 2). The results indicated that the best parameters for temperature and time were 180 °C and 60 min, respectively.

3.2. Characterization

Fluorescence spectra of the hydrogel are shown in (Fig. 3). The hydrogel displayed maximal excitation and emission wavelengths at 471 nm and 556 nm, respectively. The structure of the hydrogel used for SEM imaging is shown in (Fig. 4 a), highlighting the presence of pores in the size range between 5 and 15 μm and exhibiting discontinuous macropores with an interconnected 3D network structure. The lumpy-looking structure endows the hydrogel with the ability to absorb and hold water. The hydrogel emitted yellow-green fluorescence under an FIM, as shown in (Fig. 4 b). The two
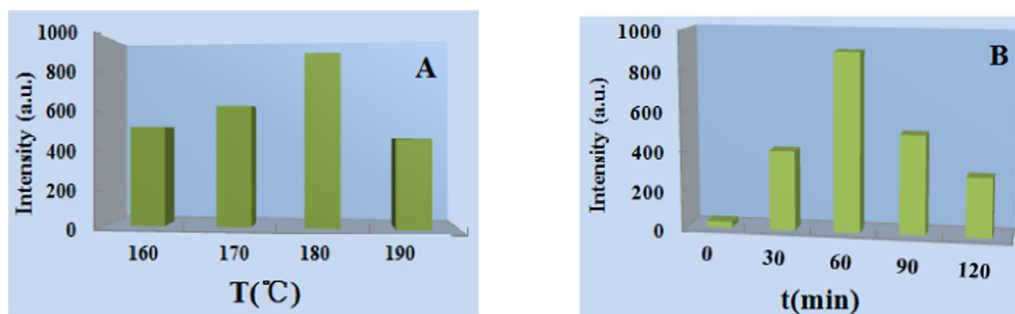
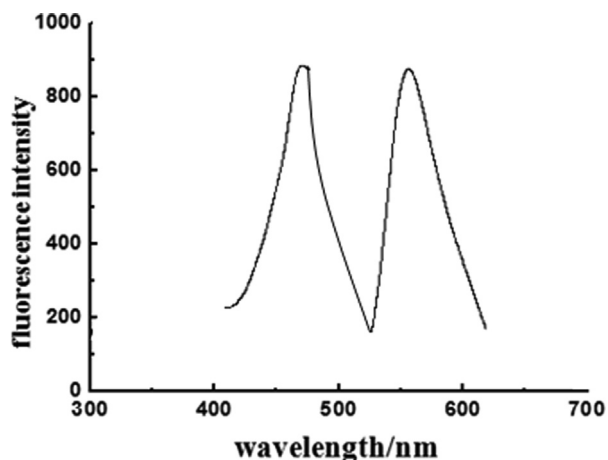**Fig. 2**   The synthesis temperature (A) and time (B).

Fig. 3   Fluorescence spectra of the hydrogel.

results coincide with each other. The hydrogel was performed camel imaged by a normal microscope, as shown in (Fig. 5).

3.3. N₂ Adsorption and desorption

Nitrogen adsorption–desorption isotherms were utilized to investigate the structure of the hydrogel. Fig. 6 depicts the characteristics of the hydrogel with macropores. The result coincided with the SEM results.

3.4. Swelling rate

The performance of hydrogel depends on the amount of water absorbed, which in turn affects the stimuli-responsiveness of the hydrogel. Water, as a common carrier of analytes, makes it easy for them to penetrate into hydrogels. Therefore, quantitative measurement of swelling can be a significance basis for assessing hydrogel performance. Weight and volume measurements are two common methods for measuring the swelling rate. The formula for swelling rate was as follows.

$$S_R = \frac{W_d - W_s}{W_s} \times 100\% \tag{1}$$

According to the equation above, the swelling rate is 680% in weight. The presence of pores in the hydrogel enable water absorption and storage. Furthermore, these results indicated that the hydrogel has great potential as a chemical sensors due to its VTP.

3.5. Sensor construction and measurement procedure

As shown in (Fig. 7), when the sensor was applied to the sample, an equal amount of hydrogel was loaded into the pipette and packed compactly with up-and-down shaking. Then, the pipette was immersed into solutions with different pH values in a 100 mL graduated cylinder. Importantly, along with the convenience of being instrument free, a calibration of the volume change of the hydrogel (Δv) against pH over a wide range
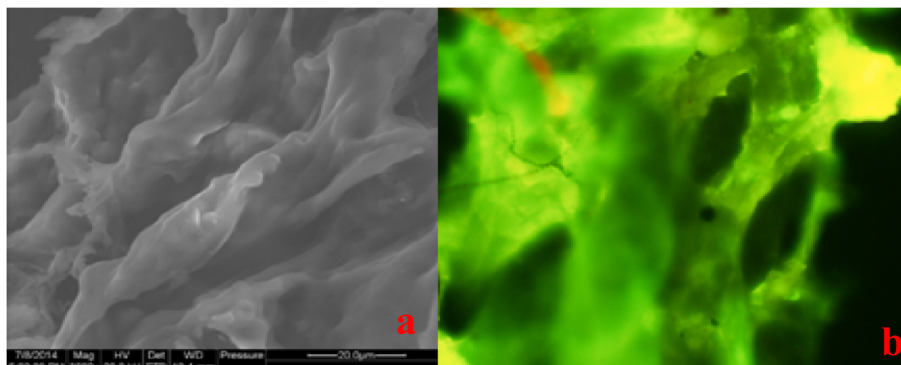

Fig. 4   Images of the fluorescent hydrogel acquired by SEM (a) and FIM (b).
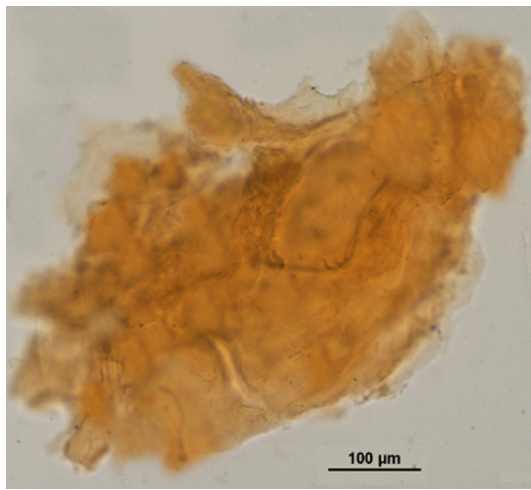
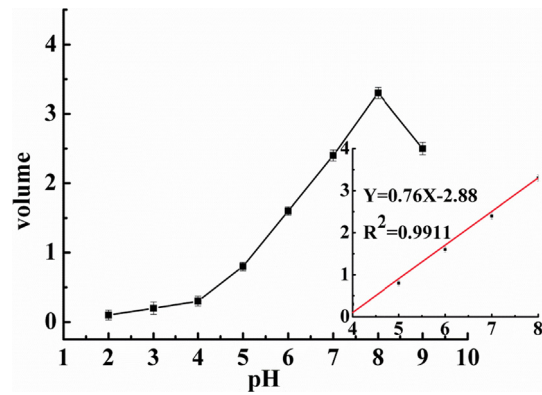**Fig. 5** Images of the hydrogel under a microscope.

Fig. 8 Sensor calibration curve of response to pH from 2 to 9 (insets are the linear plots of the volume response vs pH in the range of 4 to 8).
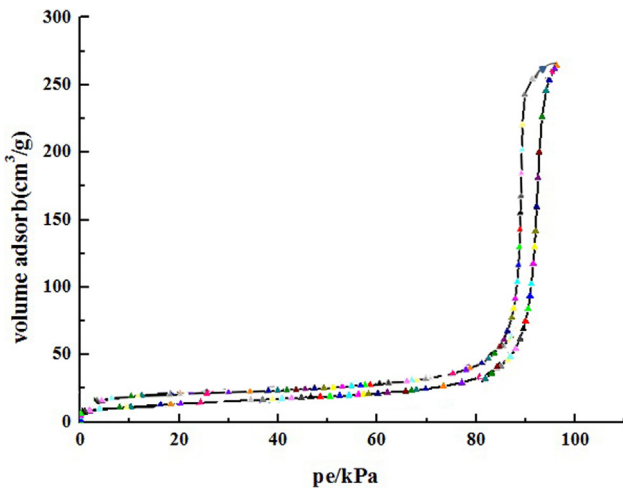

Fig. 6 Nitrogen adsorption–desorption isotherms of the hydrogel.

was established. As shown in (Fig. 8), the volume variation in the hydrogel was highly sensitive to pH. The best swelling performance of the obtained fluorescent hydrogel was at pH 8. By contrast, the volume change in the fluorescent hydrogel was almost negligible at pH 3. In the pH range from 3 to 8, the degree of swelling increased with increasing pH. When the pH of the solution was higher than 8, the degree of swelling decreased. The results demonstrated that in the range from 4 to 8, the volume change in the hydrogel had a linear correlation with pH. The developed sensor exhibited direct- reading ability, repeatability, viability, robustness, and portability, which allowed detection without any complicated processes or requisite analytical apparatus.

3.6. Scale bar

The scale bar is shown in (Fig. 9). A and B are the divided sections of a scale bar. The larger purple figures (1.5, 2.0, 2.5, 3.0) on the left side of the scale bar are the volume graduations of the pipette. The dark figures (5.76, 5.89…7.74) represent the pH value corresponding to the volume. The larger red figures (4.5, 5.0,…6.0) along the scale bar are the pH values corresponding to the volume in section B. The dark figures (0.54, 0.62…1.68) denote the volume. With the aid of the scale bar, pH could be directly and quantitatively determined with the naked eye.
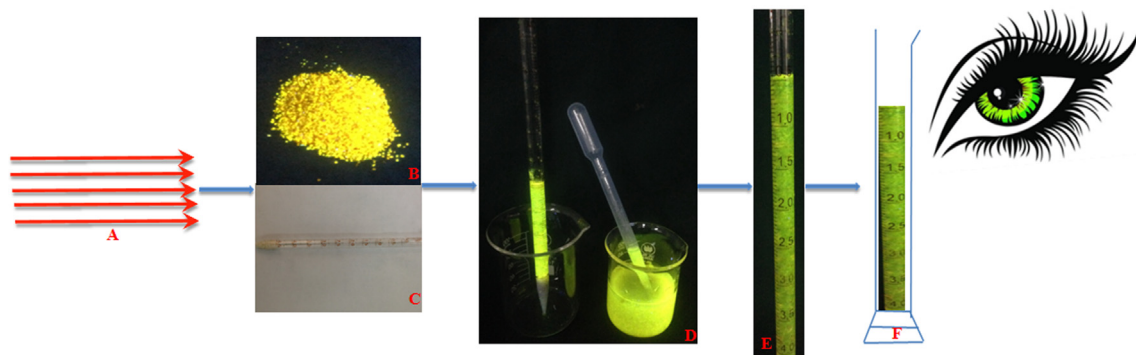

Fig. 7 The fabrication of fluorescent hydrogels towards pH detection. (A, laser engraving; B, hydrogel under fluorescence; C, pipette with its end sealed with cotton; D, fully water-swelled hydrogel used to fill the pipette; E, full of hydrogel in pipette ; F, naked eye for readout).
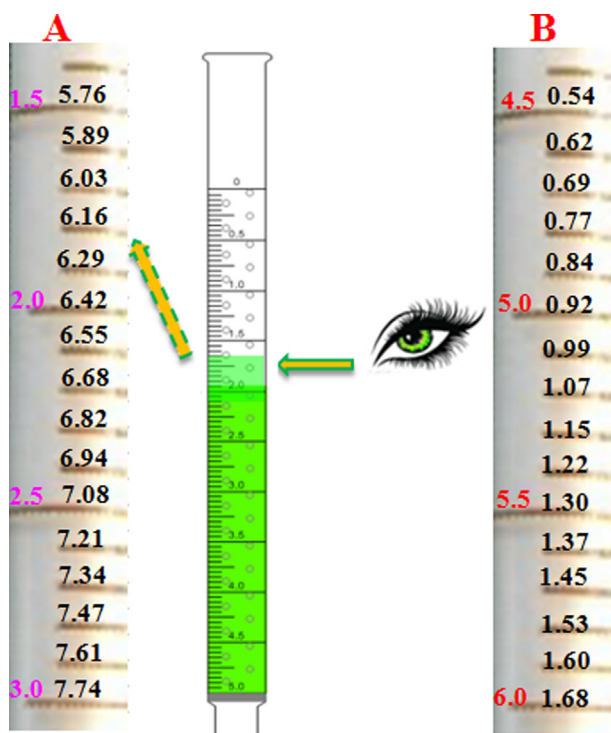
**Fig. 9** Scale bar and its use for direct pH readout.

4. Discussion

pH-sensitive polymer hydrogel sensor are classified into two groups: anionic and cationic. Anionic hydrogels have a carboxylic or sulfonic acid group, and cationic hydrogels have amines. The mechanism for the pH-dependent hydrogel volume change is illustrated in (scheme 3). The 5,6-dicarboxyl fluorescein molecules played an important role in the VPT and in the introduction of functionalization groups, such as amino and carboxyl groups.

When the pH was increased, the hydroxyl group on the xanthene ring began to ionize, and the fluorescence intensity was further enhanced. Similarly, the hydrogel volume was also greatly affected by pH. When the pH was less than 3, the amino group in the hydrogel molecular chain was protonated and became positively charged. Therefore, the electrostatic repulsion between the chains was enhanced. As a result, the hydrogel gradually swelled. In the pH range from 3 to 8, amino group protonation reduced the electrostatic repulsion between the molecular chains. However, due to the increase in hydrophobic interactions between the chains and the gradual transformation of –COOH to –COO$^-$, when the pH was further increased, the electrostatic repulsion between the molecular chains was gradually enhanced. The effect of this increase was greater than that of the weakening, so the degree of swelling in this range increased with the pH. When the pH of the solution exceeded 8, the –COO$^-$ groups in the chain enhanced the electrostatic repulsion. Due to the large number of –NH$_2$ groups under alkaline conditions, a strong interaction with Na$^+$ was induced by NaOH ionization. This effect made the hydrogel polymer chains hydrophobic at the microscale and made them swell poorly at the macroscale. As a result, a pH sensor was developed.

5. Conclusions

A thermometer-type hydrogel sensor based on volume change was reported for pH response. When the sensor was applied to different pH solutions, a volume change in hydrogel occurred due to the carboxylic and amine groups in the polymer chain. The volume change was recorded with an elaborate graduated pipette similar to a thermometer. Compared with the VPT hydrogel sensors reported previously, our sensor benefited from the approach that we developed to measure the three-dimensional volume of the hydrogel. This smart thermometer-type fluorescent sensor opened up a new route towards VPT hydrogels. The system is proposed as a competent instrument-free and lowcost, portable platform enables quantitative and sensitive assays on the scene.
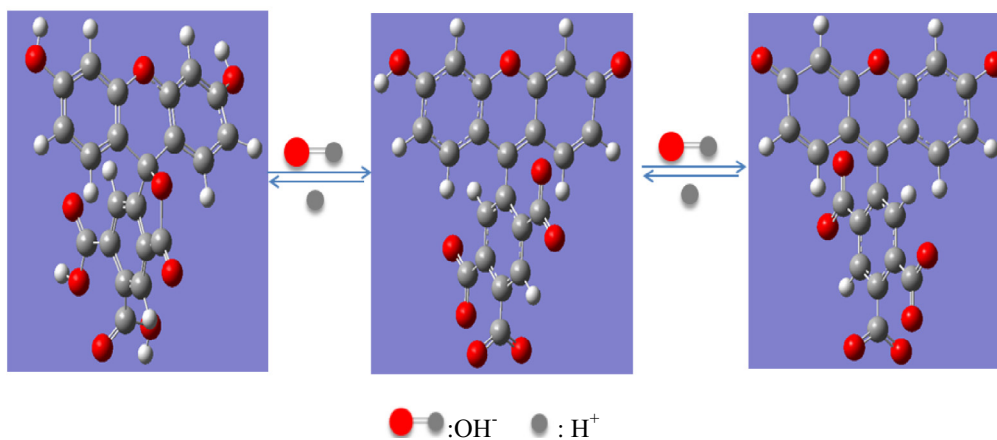
Scheme 3   The influence of pH on fluorescein.

Acknowledgments

References

Ibrahim, K., Khalid, S., Idrees, K., 2019. Nanoparticles: properties, applications and toxicities. Arab. J. Chem 12, 908–931.

Viran, P.M., Manish, P.P., 2016. Removal of some most hazardous cationic dyes using novel poly (NIPAAm/AA/N-allylisatin) nanohydrogel. Arab. J. Chem 9, 430–442.

Zhu, Z., Wu, C.C., Liu, H.P., et al, 2010. An aptamer cross-linked hydrogel as a colorimetric platform for visual detection. Angew. Chem. Int. Ed. 49, 1052–1056.

Askim, J.R., Mahmoudia, M., Suslick, K.S., 2013. Optical sensor arrays for chemical sensing: the optoelectronic nose. Chem. Soc. Rev. 42, 8649–8682.

Markus, G., Marian, S., Genger, U.R., 2016. Highly fluorescent dye–nanoclay hybrid materials made from different dye classes. Langmuir 32, 3506–3513.

Shimanovich, U., Gedanken, A., 2016. Nanotechnology solutions to restore antibiotic activity. J. Mater. Chem. B 4, 824–833.

Zhen, Q., Jesse, P., Phillip, C., Ji, H.F., 2019. Applications of highly stretchable and tough hydrogels. Polymers. 11, 1773–1788.

Si, H.P., Xing, T.L., Ding, Y.L., et al, 2019. 3D Bioprinting of the sustained drug release wound dressing with double-crosslinked hyaluronic-acid-based hydrogels. Polymers 11, 1584–1590.

Chen, G., Tang, W.W., Wang, X.H., et al, 2019. Applications of hydrogels with special physical properties in biomedicine. Polymers 11, 1420–1432.

Shao, H., Wang, C.F., Zhang, J., et al, 2014. Fabrication of reversible phase transition polymer gels toward metal ion sensing. Macromolecules 47, 1875–1881.

Wang, Y.X., Niu, J.Y., Hou, J., 2018. A novel design strategy for triple-network structure hydrogels with high-strength, tough and self-healing properties. Polymer 135, 16–24.

Zhu, Z., Guan, Z.C., Jia, S.S., et al, 2016. Au@Pt nanoparticle encapsulated target-responsive hydrogel with volumetric bar-chart chip readout for quantitative point-of-care testing. Angew. Chem. Int. Ed. 53, 12503–12510.

Kehr, N.S., 2014. Enantiomorphousperiodic pesoporous crganosilica-based nano-composite hydrogel scaffolds for cell adhesion and cell enrichment. Biomacromolecules 17, 1117–1122.

Gao, W.W., Vecchio, D., Li, J.M., 2014. Hydrogel containing nanoparticle-stabilized liposomes for topical antimicrobial delivery. ACS Nano 8, 2900–29055.

Wang, H., Gu, X.Y., Wang, C.Y., 2016. Self propelling hydrogel/emulsion hydrogel soft motors for water purification. ACS Appl. Mater Interfaces 8, 9413–9417.

Carmen, M.G.H., Guadalupe, C.P., Mauricio, A.S., et al, 2019. In situ-preparation and characterization of silver HEMA/PEGDA hydrogel matrix nanocomposites: silver inclusion studies into hydrogel matrix. Arab. J. Chem. 12, 1413–1423.

Héloïse, T.A., Wu, Z.L., Nie, Z.H., 2013. Multiple shape transformations of composite hydrogel sheets. JACS 135, 4834–4838.

Seddiki, N., Aliouche, D., 2017. Synthesis, characterization and rheological behavior of pH sensitive poly(acrylamide-co-acrylic acid) hydrogels. Arab. J. Chem. 10, 539–547.

Kuang, D.J., Wu, F., Yin, Z.P., et al, 2018. Silk fibroin/polyvinyl pyrrolidone interpenetrating polymer network hydrogels. Polymers. 10, 153–165.

Jae, S.C., Anantha, I.G., Nallal, M.K., et al, 2016. Design of graphene- and polyaniline-containing functional polymer hydrogel as a new adsorbent for removal of chromium (VI) ions. Polymers. 8, 445–456.

Cui, Y.F., Xing, Z.J., Yan, J., et al, 2018. Thermosensitive behavior and super-antibacterial properties of cotton fabrics modified with a sercin-NIPAAm-AgNPs interpenetrating polymer network hydrogel. Polymers 10, 818–830.

Sebastian, C., Torsten, R., Sebastian, S., 2016. Hybrid polymer-network hydrogels with tunable mechanical response. Polymers 8, 82–98.

Li, T.J., Tang, H., Wu, P.Y., 2015. Structural investigation of thermo-responsive poly(2-isopropyl-2-oxazoline) hydrogel across the volume phase transition. Soft Matter 11, 1911–1917.

Coukouma, A.E., Asher, S.A., 2018. Increased volume responsiveness of macroporous hydrogels. Sensor Actuat B-Chem. 255, 2900–2905.

Cheng, Y., Li, N., Wei, C.D., 2016. Effect of the TMCS/hydrogel volume ratio on physical properties of silica aerogels based on fly ash acid sludge. J. Sol-Gel Sci. Technol. 78, 279–283.

Cai, Z.Y., Luck, L.A., Punihaole, D., 2016. Photonic crystal protein hydrogel sensor materials enabled by conformationally induced volume phase transition. Chem. Sci. 7, 4557–4562.

Su, G.H., Zhou, T., Liu, X.F., 2017. Two-step volume phase transition mechanism of poly(N-vinylcaprolactam) hydrogel online-tracked by two-dimensional correlation spectroscopy. PCCP 19, 27221–27225.

Gong, X.L., Xiao, Y.Y., Pan, M., 2016. pH- and thermal-responsive multishape memory hydrogel. ACS Appl. Mater. Interfaces 8, 27432–27436.

Wang, X.Q., Liu, X.Y., Wang, X.G., 2014. Hydrogel diffraction grating as sensor: a tool for studying volumephase transition of thermo-responsive hydrogel. Sens. Actuators, B 204, 611–617.

Yu, C., Kai, R., Yang, D., et al, 2018. Bilayer-type fluorescence hydrogels with intelligent response serve as temperature/pH driven soft actuators. Sensor Actuat B-Chem. 255, 3117–3123.

Deng, K.F., Bellmann, C., Fu, Y.X., 2018. Miniaturized force-compensated hydrogel-based pH sensors. Sensor Actuat B-Chem. 255, 495–500.

Mistlberger, G., Pawlak, M., Bakker, E., et al, 2015. Photodynamic optical sensor for buffer capacity and pH based on hydrogel-incorporated spiropyran. Chem. Commun. 51, 4172–4176.

Sun, Y.W., Zhang, Y.P., Liu, J.J., et al, 2016. Integrated microfluidic device for the spherical hydrogel pH sensor fabrication. RSC Adv. 6, 11204–11209.

Satyendra, K.M., Banshi, D.G., 2013. Surface plasmon resonance based fiber optic pH sensor utilizing Ag/ITO/Al/hydrogel layers. Plasmonics 138, 2640–2646.